

from other forms of reduced carbon (for example, soot) that have been observed at the K-T boundary (25). The $\delta^{13}\text{C}$ values are unusual but not impossible for kimberlite or lamproite diamonds (24), but the C/N ratio of 114 is much greater than that seen for any deep-Earth or laboratory-synthesized diamonds (26). Indeed, the variations in $\delta^{13}\text{C}$, $\delta^{15}\text{N}$ abundance, and $\delta^{15}\text{N}$ indicate the presence of more than one C source and mechanism. Perhaps coincidentally, the $\delta^{13}\text{C}$ of the diamonds is close to the typical isotopic composition of macromolecular or amorphous C from carbonaceous chondrites (27). Although most larger shocked diamonds are hexagonal in structure, diamonds produced by the explosive detonation of TNT were also found to be cubic and to have morphologies, grain size, and high N contents (28) similar to those of the K-T diamonds.

REFERENCES AND NOTES

1. L. W. Alvarez, W. Alvarez, F. Asaro, H. V. Michel, *Science* **208**, 1095 (1980).
2. O. Eugster, J. Geiss, U. Krahenbuhl, *Earth Planet. Sci. Lett.* **74**, 27 (1985).
3. F. T. Kyte, J. Smit, J. T. Wasson, *ibid.* **73**, 183 (1985); G. I. Bekov, V. S. Letokhov, V. N. Radaev, D. D. Badyukov, M. A. Nazarov, *Nature* **332**, 146 (1988); E. Doehe and S. V. Margolis, in *Global Catastrophes in Earth History: An Interdisciplinary Conference on Impacts, Volcanism, and Mass Mortality*, V. L. Sharpton and P. D. Ward, Eds. (Geological Society of America, Boulder, CO, 1990), p. 367.
4. F. E. Lichte *et al.*, *Nature* **322**, 816 (1986).
5. D. B. Carlisle and D. R. Braman, *ibid.* **352**, 708 (1991).
6. R. S. Lewis, T. Ming, J. F. Wacker, E. Anders, E. Steel, *ibid.* **326**, 160 (1987).
7. G. R. Huss, *ibid.* **347**, 159 (1990); C. M. O. Alexander, J. W. Arden, R. D. Ash, C. T. Pillinger, *Earth Planet. Sci. Lett.* **99**, 220 (1990).
8. S. S. Russell, J. W. Arden, C. T. Pillinger, *Science* **254**, 1188 (1991).
9. P. K. Swart, M. M. Grady, C. T. Pillinger, R. S. Lewis, E. Anders, *ibid.* **220**, 406 (1983); R. S. Lewis, E. Anders, I. P. Wright, S. J. Norris, C. T. Pillinger, *Nature* **305**, 767 (1983).
10. Light-element isotopic compositions are expressed as δ values where, for example:

$$\delta^{15}\text{N} = \left[\frac{(^{15}\text{N}/^{14}\text{N})_{\text{sample}}}{(^{15}\text{N}/^{14}\text{N})_{\text{standard}}} - 1 \right] \times 1000$$
standards are for N, air, and C, a belemnite fossil, from the Pee Dee formation.
11. Two clay layers can be identified at some K-T boundary sites. The upper layer, termed the fireball layer, is typically 2 to 4 mm thick, occurs globally, and contains anomalously high amounts of siderophile and chalcophile trace elements, shocked minerals, and spherules with spinels. It is thought to be formed by vaporization of the projectile and target. On and near North America, a clay layer up to 50 cm thick and with similar impact-related constituents underlies the fireball layer. Termed the ejecta layer, it may represent geographically restricted facies of less energetic ejecta; A. R. Hildebrand and W. V. Boynton, *Science* **248**, 843 (1990); W. Alvarez *et al.*, *Geology* **20**, 697 (1992); C. C. Swisher III *et al.*, *ibid.* **257**, 954 (1992).
12. J. W. Arden, R. D. Ash, M. M. Grady, I. P. Wright, C. T. Pillinger, *Lunar Planet. Sci.* **20**, 21 (1989).
13. P. K. Swart, M. M. Grady, C. T. Pillinger, *Meteoritics* **18**, 137 (1983).
14. R. H. Carr, I. P. Wright, A. W. Joines, C. T. Pillinger, *J. Phys. E* **19**, 798 (1986).
15. R. D. Ash, J. W. Arden, M. M. Grady, I. P. Wright, C. T. Pillinger, *ibid.* **21**, 870 (1988); P. D. Yates, I. P. Wright, C. T. Pillinger, *Chem. Geol.* **101**, 81 (1992).
16. S. J. Prosser, I. P. Wright, C. T. Pillinger, *Chem. Geol.* **83**, 71 (1990); I. P. Wright, S. R. Boyd, I. A. Franchi, C. T. Pillinger, *J. Phys. E* **21**, 865 (1988).
17. I. P. Wright and C. T. Pillinger, *U. S. Geol. Surv. Bull.* **1890**, 9 (1989).
18. S. S. Russell, J. W. Arden, C. T. Pillinger, *Meteoritics* **27**, 283 (1992).
19. D. B. Carlisle, *Nature* **357**, 119 (1992).
20. I. P. Wright, *ibid.* **358**, 198 (1992).
21. S. S. Russell, C. T. Pillinger, J. W. Arden, M. R. Lee, U. Ott, *Science* **256**, 206 (1992).
22. G. Vdovykin, in *Advances in Organic Geochemistry*, P. A. Shenk and I. Havenaar, Eds. (Pergamon, Oxford, 1968), p. 593; *Space Sci. Rev.* **10**, 483 (1970).
23. M. M. Grady, I. P. Wright, P. K. Swart, C. T. Pillinger, *Geochim. Cosmochim. Acta* **49**, 903 (1985).
24. E. M. Galimov, *ibid.* **55**, 1697 (1991).
25. W. S. Wolbach, I. Gilmour, E. Anders, C. J. Orth, R. R. Brooks, *Nature* **334**, 665 (1988); I. Gilmour, W. S. Wolbach, E. Anders, in *Catastrophes and Evolution: Astronomical Foundations*, S. V. M. Clube, Ed. (Cambridge Univ. Press, Cambridge, 1989), pp. 195–213.
26. S. R. Boyd *et al.*, *Earth Planet. Sci. Lett.* **86**, 341 (1987); S. R. Boyd, C. T. Pillinger, H. J. Milldege, M. J. Mendelsohn, M. Seal, *Nature* **331**, 604 (1988).
27. J. W. Smith and I. R. Kaplan, *Science* **167**, 1367 (1970).
28. S. S. Russell, A. V. Fisenko, C. T. Pillinger, unpublished results.
29. We thank B. Bohor, A. R. Hildebrand, and A. Montanari for the samples that made this investigation possible. We also thank G. R. Huss for a constructive review. Supported by the Royal Society, Science and Engineering Research Council, and the Natural Environment Research Council.

8 June 1992; accepted 15 September 1992

A High-Resolution Record of Holocene Climate Change in Speleothem Calcite from Cold Water Cave, Northeast Iowa

Jeffrey A. Dorale, Luis A. González,* Mark K. Reagan, David A. Pickett, Michael T. Murrell, Richard G. Baker

High-precision uranium-thorium mass spectrometric chronology and ^{18}O - ^{13}C isotopic analysis of speleothem calcite from Cold Water Cave in northeast Iowa have been used to chart mid-Holocene climate change. Significant shifts in $\delta^{18}\text{O}$ and $\delta^{13}\text{C}$ isotopic values coincide with well-documented Holocene vegetation changes. Temperature estimates based on $^{18}\text{O}/^{16}\text{O}$ ratios suggest that the climate warmed rapidly by about 3°C at 5900 years before present and then cooled by 4°C at 3600 years before present. Initiation of a gradual increase in $\delta^{13}\text{C}$ at 5900 years before present suggests that turnover of the forest soil biomass was slow and that equilibrium with prairie vegetation was not attained by 3600 years before present.

Midcontinental climatic records with decade resolution have been difficult to obtain beyond the last two millennia. A geologic record that received much attention in the 1970s is that preserved in the carbon and oxygen isotopic composition of speleothem (cave) calcite (1). Although this method has been used successfully to interpret climatic changes, the large sample sizes required for analysis precluded the routine use of speleothems for high-resolution paleoclimatic studies. Improvements in mass spectrometric techniques in the last decade now allow uranium series age-dating of subgram-sized carbonate samples with extremely small analytical errors (2–4). Because many

continental regions contain karsted limestone terrains, the possibility of using speleothems for paleoclimatic reconstruction deserves renewed attention. In this study we analyze calcite from a stalagmite to demonstrate the feasibility of extracting a high-resolution climatic record from speleothem calcite.

Thirty $\delta^{18}\text{O}$ and $\delta^{13}\text{C}$ analyses (5) were obtained from stalagmite 1s from Cold Water Cave, northeastern Iowa ($43^\circ 28' \text{N}$, $91^\circ 58' \text{W}$) (Fig. 1). Conditions in Cold Water Cave are ideal for isotopic equilibrium deposition of calcite (6). Stalagmite 1s was cored from the bottom up to within a centimeter of the top surface with a 2.5-cm-diameter coring apparatus (7). The core was split and thin sections of core material were inspected by standard polarizing light microscopy to evaluate the possibility that the calcite had recrystallized. We extracted materials for stable isotopic, alpha, and mass spectrometric U-Th analysis (8) from the split and polished core using a carbide dental burr on a microscope-mounted drill

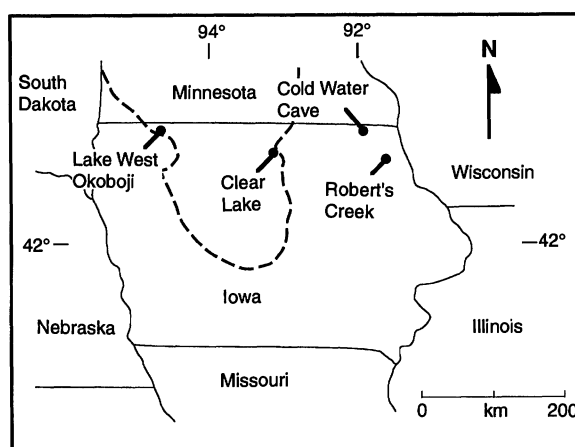
J. A. Dorale, Department of Geology, University of Iowa, Iowa City, IA 52242.

L. A. González, M. K. Reagan, R. G. Baker, Department of Geology and Center for Global and Regional Environmental Research, University of Iowa, Iowa City, IA 52242.

D. A. Pickett and M. T. Murrell, Isotope Sciences Group, Los Alamos National Laboratory, Los Alamos, NM 87545.

*To whom correspondence should be addressed.

Fig. 1. Map of Iowa and surrounding region showing the location of Cold Water Cave and sites of previous palynological studies [Lake West Okoboji (26), Clear Lake (27), and Robert's Creek (28)]. Dashed line shows the maximum extent of late Wisconsin glaciation.



assembly. The sampling resolution for U-Th analysis ranged from 40 to 10 layers (Table 1); growth banding is assumed to represent annual events, and resolution is better than 50 years for all samples. With the exception of those samples analyzed from a split of the U-Th samples, the samples for C and O isotope analysis ranged from a single layer to a maximum of nine layers (Table 2).

The mass and alpha spectrometric ages agreed within errors (Table 1), and all ages are in correct stratigraphic order. The data and the fresh appearance of the calcite suggest that significant postformational alteration of stalagmite 1s did not occur. The six ages cover 135 mm of core and range from 7774 ± 42 to 1147 ± 7 years before present (YBP). The lack of evidence of depositional discontinuities suggests that growth was continuous through the life of the speleothem. Growth rates for the assumption that growth was uninterrupted between dated intervals range from 14 to 43 mm per 1000 years.

The $\delta^{18}\text{O}$ values range from 23.60 to 26.11 per mil, and $\delta^{13}\text{C}$ values range from -5.02 to -9.01 per mil (Table 2). The observed variability can be divided into three distinct stages (Fig. 2). Stage 1 extends from 7770 to 5900 YBP, during which time both $\delta^{18}\text{O}$ and $\delta^{13}\text{C}$ values remained essen-

tially constant. During stage 1, $\delta^{18}\text{O}$ values averaged 24.76 per mil and $\delta^{13}\text{C}$ values averaged -8.58 per mil. Stage 2 is characterized by a significant excursion to higher $\delta^{18}\text{O}$ and $\delta^{13}\text{C}$ values for the period between 5900 and 3600 YBP. At the beginning of stage 2, $\delta^{18}\text{O}$ values rose abruptly to an average value of 25.81 per mil. The increase in $\delta^{13}\text{C}$ values during stage 2 was gradual, reaching a maximum of -5.02 per mil at 3600 YBP. During stage 3 (3600 to 1150 YBP), both $\delta^{18}\text{O}$ and $\delta^{13}\text{C}$ returned to lower values. The $\delta^{18}\text{O}$ values dropped abruptly to an average of 24.14 per mil, whereas $\delta^{13}\text{C}$ values steadily declined to a minimum of -7.96 per mil. The timing of the stage 1-stage 2 transition is tightly constrained by coincidence with date MS-3, at 5890 ± 42 YBP. The timing of the stage 2-stage 3 transition has been estimated by linear interpolation between dates MS-1 and MS-2 to be at about 3600 ± 200 YBP.

The stable isotopic composition of calcite is determined by the isotopic composition of its precipitating parent fluid and the conditions of formation (1). Vadose ground waters acquire high CO_2 concentrations in the soil atmosphere and dissolve carbonate bedrock en route to underlying caves. Because the partial pressure of CO_2 in a cave is generally less than that of the soil atmosphere, calcite-saturated seepage waters en-

tering a cave lose CO_2 , and calcite deposition occurs. Isotopic equilibrium is maintained between calcite and parent fluids only when dissolved CO_2 is lost at a slow enough rate to maintain equilibrium between HCO_3^- , CO_3^{2-} , and CO_2 (aqueous) (9). These conditions exist in areas of caves removed from openings, where air circulation is minimal and both the high relative humidity and partial pressure of CO_2 remain stable throughout the year (9). Conditions in Cold Water Cave are ideal for equilibrium deposition of calcite; average depth is about 30 m, and there are no known natural entrances other than where the cave stream exits the 8-km-long cavern through a siphon at the base of a cliff.

Equilibrium $\delta^{18}\text{O}$ compositions in calcite speleothems ($\delta^{18}\text{O}_c$) are determined by the $\delta^{18}\text{O}$ of speleothem-forming waters ($\delta^{18}\text{O}_w$) and the temperature of deposition (1). In temperate regions, the $\delta^{18}\text{O}$ of deep vadose ground waters closely reflects the mean annual $\delta^{18}\text{O}$ of meteoric precipitation ($\delta^{18}\text{O}_p$) (10, 11). Because of the short residence time of water in the vadose zone, in the absence of metastable mineralogies in the overlying rocks, significant shifts in the $\delta^{18}\text{O}$ composition of water seeping into caves cannot be induced by rock-water interactions (11–14). Although the isotopic composition of individual precipitation events may vary considerably, annual average $\delta^{18}\text{O}_p$ values remain quite constant from year to year (15) and at the continental scale correlate positively with mean annual temperature (16, 17).

Ambient temperatures in poorly ventilated areas of deep caves (>11 m) are generally quite stable, reflecting mean surface temperature over several years (18). The temperature dependence of oxygen isotopic fractionation between calcite and water is such that colder temperatures result in greater fractionation and heavier calcite $\delta^{18}\text{O}$ values relative to water $\delta^{18}\text{O}$, whereas warmer temperatures result in lesser fractionation (19). Thus, temperature affects speleothem $\delta^{18}\text{O}_c$ compositions both by controlling the isotopic fractionation be-

Table 1. Uranium and thorium mass spectrometric analytical results for stalagmite 1s. Analytical errors are 2σ of the mean. Errors of ages are based on this analytical precision. Corrections for detrital ^{230}Th were calculated with data from the insoluble residue in sample MS-1 (8). The

correction is negligible for MS-5 and MS-6, within the range of analytical error for MS-2, MS-3, and MS-4, and about 2% for MS-1. The decay constants used are $9.1952 \times 10^{-6} \text{ year}^{-1}$ for ^{230}Th and $2.835 \times 10^{-6} \text{ year}^{-1}$ for ^{234}U .

Sample	Distance from bottom (in mm)	Number of layers sampled	U (ppm)	$^{234}\text{U}/^{238}\text{U}$ (atomic)	% error	$^{230}\text{Th}/^{232}\text{Th}$ (atomic)	$^{230}\text{Th}/^{238}\text{U}$ (activity)	% error	$^{230}\text{Th}/^{234}\text{U}$ age (corrected) (years BP)	Initial ($^{234}\text{U}/^{238}\text{U}$) (activity)	Alpha age
MS-1	146.0	40	1.082	1.098×10^{-4}	0.28	1.218×10^{-4}	0.02151	0.49	1147 ± 07	2.011	
MS-2	94.5	14	1.422	1.059×10^{-4}	0.38	5.263×10^{-4}	0.08317	0.45	4742 ± 31	1.948	4740 ± 1860
MS-3	70.5	12	1.001	1.061×10^{-4}	0.46	4.241×10^{-4}	0.1032	0.47	5890 ± 42	1.956	
MS-4	56.5	14	0.919	1.071×10^{-4}	0.28	7.662×10^{-4}	0.1111	0.46	6306 ± 38	1.975	
MS-5	37.5	10	1.352	1.081×10^{-4}	0.33	1.471×10^{-2}	0.1279	0.45	7243 ± 49	1.996	
MS-6	14.0	10	1.787	1.083×10^{-4}	0.32	1.929×10^{-2}	0.1373	0.35	7774 ± 42	2.001	8870 ± 1180

tween calcite and water and by influencing the isotopic composition of precipitation. Because the effects of temperature on $\delta^{18}\text{O}_c$ and $\delta^{18}\text{O}_p$ are opposite (that is, warmer temperatures lead to lower $\delta^{18}\text{O}_c$ and higher $\delta^{18}\text{O}_p$), the effect of temperature on speleothem ^{18}O fractionation is masked by the temperature effect on $\delta^{18}\text{O}_p$.

The dissolved carbon species in cave waters are derived from soil CO_2 and the carbonate bedrock (20). In temperate climates, soil CO_2 is largely produced by the decomposition of organic matter and by plant root respiration (soil respiration), and the $\delta^{13}\text{C}$ composition of soil CO_2 is related to the type of vegetation occupying the land surface (21). Plants that utilize the Calvin, or C_3 , photosynthetic pathway have $\delta^{13}\text{C}$ compositions that average about -26 per mil, whereas plants utilizing the Hatch-Slack, or C_4 , pathway have $\delta^{13}\text{C}$ compositions that average -13 per mil (22). C_3 plants, which include almost all trees and many grasses, are better adapted

to cooler, moister growing seasons (23). Many C_4 plants are grasses that have evolved to take advantage of hot, dry environmental conditions (23). The percentage of C_4 plants for a region is well correlated with minimum temperatures during the growing season (24).

Soil seepage waters acquire their initial $\delta^{13}\text{C}$ signatures from soil CO_2 and are modified when carbonate bedrock [-3 per mil to $+4$ per mil (25)] is dissolved en route to underlying caves. Changes in the $\delta^{13}\text{C}$ compositions of cave seepage waters are controlled by changes in the $\delta^{13}\text{C}$ composition of soil CO_2 or changes in the bedrock (that is, rock thickness and fluid pathways, or both). In the time scale of hundreds to thousands of years, major changes in the thickness of overlying carbonate bedrock and alteration of vadose fluid pathways are unlikely, and changes in cave seepage water $\delta^{13}\text{C}$ compositions are most likely the result of changes in the soil atmosphere.

In the western and central portions of

Iowa, documented changes in vegetation for the last 11,000 years suggest that the climate was significantly drier and perhaps warmer between 8000 to 3000 RCYBP (radiocarbon years before present) (26, 27). In contrast, humid climate persisted in the eastern part of the state until 5500 RCYBP, requiring a sharp mid-Holocene climatic boundary between central and eastern Iowa (27, 28). In particular, recent evidence from Robert's Creek (see Fig. 1), located 60 km southeast of Cold Water Cave, indicates the replacement of forest by prairie vegetation at about 6200 YBP (29) and that those conditions prevailed until about 3200 YBP (30). The coincidence in timing of the observed variations in stalagmite 1s with the timing of vegetation change at Robert's Creek argues strongly for climate-induced change in stalagmite 1s isotopic composition.

The most likely explanation of the stage 2 increase in $\delta^{18}\text{O}_c$ of stalagmite 1s is that $\delta^{18}\text{O}_p$ increased as the mean annual temperature increased. Although the exact $\delta^{18}\text{O}_p$ -temperature relation for northeastern Iowa is not known, other documented relations are available (10, 16, 17). The relation of Dansgaard (16) yields values similar to those of present-day precipitation (31).

If Dansgaard's (16) $\delta^{18}\text{O}$ -temperature relation has held for northeast Iowa for the last 8000 years, the temperature shifts required to cause the observed $\delta^{18}\text{O}_c$ change in stalagmite 1s can be estimated (Table 2). The calcite-water oxygen isotopic fractionation relation (32) and the $\delta^{18}\text{O}_p$ -temperature relation (16) can be combined as

$$\delta^{18}\text{O}_c = \left[\frac{2780}{(273.15 + t)^2} \right] - 0.00289 \times (0.695t + 986.4) - 1000$$

(where t is in $^{\circ}\text{C}$).

Solving for temperature for the observed $\delta^{18}\text{O}_c$ results in good agreement between the calculated present-day $\delta^{18}\text{O}_c$ (with present-day mean t of 7.3°C) of 24.18 per mil and the observed stage 3 $\delta^{18}\text{O}_c$ average of 24.14 per mil (Table 2). Use of the observed stage 1 average $\delta^{18}\text{O}_c$ values to constrain temperature changes yields a mean annual temperature of about 8.6°C during that time. For stage 2, a mean annual temperature of about 10.8°C is required to produce the average $\delta^{18}\text{O}_c$ value of 25.81 per mil. Thus, the mid-Holocene stage 2 isotopic excursion represents a warming of almost 3°C from stage 1 conditions, and the late-Holocene stage 3 period experienced a drop of almost 4°C in mean annual temperature from stage 2 conditions.

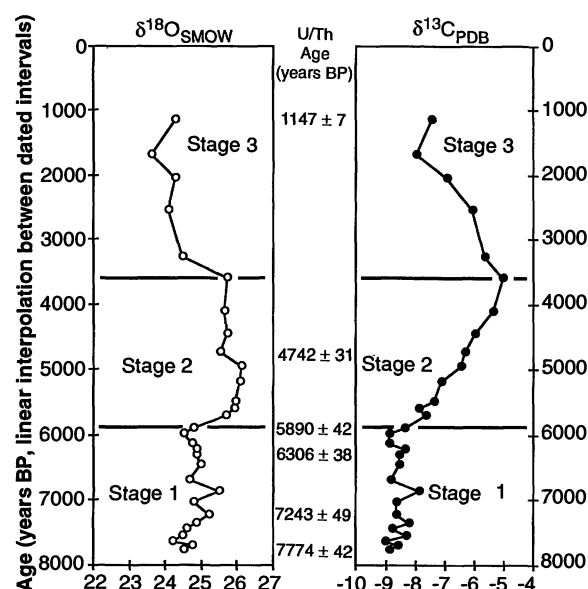
Two alternative explanations for the data are less favorable. First, the observed increase of $\delta^{18}\text{O}_c$ values can be explained by colder mean annual temperature with no change in $\delta^{18}\text{O}_p$. Temperatures calculated

Table 2. Stable isotope samples. The age of individual samples was determined by linear interpolation between dated intervals. The calculated temperature was obtained by iterative solution to the combined calcite fractionation equation (32) and $\delta^{18}\text{O}_p$ -temperature relation (16). The calculated $\delta^{18}\text{O}_p$ was obtained with the use of Dansgaard's $\delta^{18}\text{O}_p$ -temperature relation (16).

Distance from bottom (in mm)	Number of layers sampled	$\delta^{13}\text{C}_c$ (PDB)	$\delta^{18}\text{O}_c$ (SMOW)	Interpolated age (YBP)	Calculated t ($^{\circ}\text{C}$)	Calculated $\delta^{18}\text{O}_p$ (SMOW)
Stage 3 (Age range, 1150 to 3600 YBP; averages, $\delta^{18}\text{O}_c = 24.14$, $t = 7.2$, $\delta^{18}\text{O}_p = -8.6$)						
146.0	40	-7.46	24.28	1147*	7.5	-8.4
138.5	8	-7.96	23.60	1671	6.0	-9.4
133.0	8	-6.92	24.28	2054	7.5	-8.4
126.0	9	-6.10	24.08	2543	7.1	-8.7
115.5	6	-5.64	24.46	3276	7.9	-8.1
Stage 2 (Age range, 3600 to 5900 YBP; averages, $\delta^{18}\text{O}_c = 25.81$, $t = 10.8$, $\delta^{18}\text{O}_p = -6.1$)						
111.0	8	-5.02	25.73	3590	10.6	-6.2
103.5	4	-5.36	25.63	4114	10.4	-6.4
98.5	4	-5.97	25.71	4463	10.6	-6.2
94.5	14	-6.30	25.52	4742*	10.2	-6.5
90.0	4	-6.48	26.11	4957	11.5	-5.6
85.0	3	-7.12	26.08	5196	11.4	-5.7
79.0	6	-7.38	25.93	5483	11.1	-5.9
76.5	6	-7.87	25.91	5603	11.0	-5.9
74.5	5	-7.63	25.65	5699	10.5	-6.3
Stage 1 (Age range, 5900 to 7770 YBP; averages, $\delta^{18}\text{O}_c = 24.76$, $t = 8.6$, $\delta^{18}\text{O}_p = -7.7$)						
70.5	12	-8.34	24.78	5890*	8.6	-7.6
67.0	5	-8.87	24.51	5994	8.0	-8.0
62.0	3	-8.88	24.74	6143	8.5	-7.7
59.5	4	-8.35	24.84	6217	8.7	-7.5
56.5	14	-8.55	24.84	6306*	8.7	-7.5
53.5	7	-8.56	24.98	6454	9.0	-7.3
48.5	3	-8.83	24.67	6701	8.4	-7.8
45.0	2	-7.87	25.47	6873	10.1	-6.6
41.5	1	-8.63	24.78	7046	8.6	-7.6
37.5	10	-8.64	25.22	7243*	9.6	-7.0
32.5	1	-8.23	24.85	7356	8.8	-7.5
28.5	1	-8.81	24.56	7446	8.1	-7.9
24.0	2	-8.30	24.48	7548	7.9	-8.1
20.0	1	-9.01	24.20	7638	7.3	-8.5
17.0	1	-8.60	24.73	7706	8.5	-7.7
14.0	8	-8.87	24.51	7774*	7.2	-8.6

*Dated interval.

Fig. 2. Oxygen and carbon isotopic composition of stalagmite 1s versus interpolated age. SMOW, standard mean ocean water; PDB, Pee Dee belemnite standard.



for the assumption that $\delta^{18}\text{O}_p$ has remained constant for the last 8000 years suggest a mean annual temperature close to 0°C during stage 2, a drop in temperature of at least 7°C . The interpretation of a significantly colder period is not consistent with other paleoenvironmental studies for the region (33). Given that for modern precipitation, colder temperatures are correlated with lower $\delta^{18}\text{O}_p$ values, it seems unlikely that $\delta^{18}\text{O}_p$ would be unaffected by a climate-induced cooling.

The second explanation attributes the increase in $\delta^{18}\text{O}_c$ to an increase in the $\delta^{18}\text{O}$ of the vapor source or a change in the vapor source. In the Midwest, three air masses dominate at present (34): (i) dry Pacific air; (ii) dry Arctic air; and (iii) moist Gulf of Mexico air, with precipitation derived almost entirely from Gulf air. Because the ^{18}O composition of the oceans has become lighter in the last 18,000 years (35), it is unlikely that Gulf vapor became heavier. A change in the vapor source is unlikely because the $\delta^{18}\text{O}$ composition of Pacific and Arctic air masses is extremely light compared to Gulf-derived precipitation (16).

The prairie invasion throughout much of the Midwest generated a significant increase in the fraction of C_4 vegetation and must have been accompanied by a corresponding enrichment of soil CO_2 and soil water $\delta^{13}\text{C}$ values. At Robert's Creek, the change from forest to prairie occurred at 6200 YBP and from prairie to savanna at 3200 YBP. For stalagmite 1s, the stage 2 onset of a gradual $\delta^{13}\text{C}_c$ excursion to higher values occurs at about 5900 YBP and begins to change back to lower values at about 3600 YBP. It seems likely that the increase in $\delta^{13}\text{C}_c$ values during stage 2 is the result of an increased proportion of C_4 plants that occupied the land surface over Cold Water Cave.

The gradual shift in $\delta^{13}\text{C}_c$ values for stalagmite 1s during both stage 2 and stage 3 might suggest a continuous and gradual change in the proportion of C_3 to C_4 vegetation since 5900 YBP. However, the abrupt $\delta^{18}\text{O}_c$ shifts at the beginning of stages 2 and 3 at 5900 and 3600 YBP provide strong evidence that the transitions in climate were rapid. The coincidence in timing of the abrupt shifts in $\delta^{18}\text{O}_c$ with the onset of gradual changes in $\delta^{13}\text{C}_c$ also suggests that vegetation changes were rapid. The apparent absence of any lag time between the $\delta^{18}\text{O}_c$ shift and the onset of the $\delta^{13}\text{C}_c$ change suggests that a change in the C_4 fraction of vegetation is incorporated into the soil atmosphere in less than a hundred years, and possibly within a few decades. Chumbley and others (28) have also suggested that at Robert's Creek, the invasion of forest by prairie was rapid and probably complete within less than 100 years.

The gradual, but large, change of $\delta^{13}\text{C}_c$ versus the abrupt change of $\delta^{18}\text{O}_c$ and vegetation can be accounted for by slow turnover rates of the soil organic matter, which have been estimated to be on the order of hundreds to thousands of years in deeper soil profiles (36, 37). Although the mid-Holocene vegetational successions above Cold Water Cave likely were rapid, turnover of the total soil biomass was slow, reflecting a replacement of C_3 plant biomass by C_4 during stage 2 and the reverse during stage 3. The continuous change of $\delta^{13}\text{C}_c$ during stage 2 implies that residual soil organic matter from stage 1 vegetation was still contributing to the total soil biomass at least until the end of stage 2, and likely into stage 3 as well, because no equilibrium condition had been achieved by that time.

The interpretation of a mid-Holocene warm and dry period in northeast Iowa is in

strong agreement with most Midwest paleoenvironmental studies. Although the "prairie peninsula" was believed to have extended far into Indiana and Ohio during this time (38), the recent work at Robert's Creek indicates that prairie arrived in northeast Iowa at 6200 YBP, much later than previously thought (28). The progressive desiccation began before 11,000 YBP in South Dakota (39) and gradually extended eastward, with the arrival of prairie at Lake West Okoboji in western Iowa (Fig. 1) at about 9900 YBP (26) and at Clear Lake in central Iowa (Fig. 1) at about 8800 YBP (27). Mesic forest species were replaced by more xeric types sometime after 6300 YBP in southern Wisconsin (40).

This recent evidence led Baker and others (40) to conclude that a sharp climatic gradient must have existed between central and eastern Iowa during the early to mid-Holocene similar to the present-day sharp climatic boundary in northwestern Minnesota that controls an abrupt ecotone, from prairie to savanna to deciduous forest to conifer hardwood forest, in a distance of 50 km (41). Baker and others (40) suggest that the expansion of prairie during the early Holocene followed an eastward advance of increasingly frequent summer Pacific air. In northeastern Iowa (Robert's Creek), humid air from the Gulf of Mexico blocked the encroachment of Pacific air between 8800 to 6200 YBP (stage 1). By 5400 YBP a decreasing frequency of Gulf air allowed the advance of dry Pacific air and the subsequent inception of prairie (stage 2). By 3000 YBP, a greater summer frequency of Arctic air led to the return of forest vegetation in much of the Midwest (40) and the cooler temperatures of stage 3.

The high-resolution chronology of stalagmite 1s provides additional and more precise constraint on the timing of Holocene climate evolution in the Midwest. The advance of dry Pacific air reached Cold Water Cave at 5900 YBP. Given the errors on the radiocarbon ages and that each dated deposit at Robert's Creek represents a period of 200 to 300 years (42), the timing of arrival of dry Pacific air at these two sites is essentially the same. Prairie reached Clear Lake, 125 km southwest of Cold Water Cave, about 3000 years before reaching Cold Water Cave. Furthermore, the late Holocene advance of summer Arctic air that led to the termination of prairie at Robert's Creek around 3200 YBP may have reached Cold Water Cave 200 to 400 years previously.

REFERENCES AND NOTES

1. H. P. Schwarcz, in *Handbook of Environmental Isotope Geochemistry: The Terrestrial Environment, Part B*, P. Fritz and J. C. Fontes, Eds. (Elsevier, New York, 1986), pp. 397-421.
2. R. L. Edwards, J. H. Chen, G. J. Wasserburg,

- Earth Planet. Sci. Lett.* **81**, 175 (1987).
3. W.-X. Li *et al.*, *Nature* **339**, 534 (1989).
 4. E. Bard, B. Hamelin, R. G. Fairbanks, A. Zindler, *ibid.* **345**, 405 (1990).
 5. Stable isotopic analyses were performed at the Univ. of Michigan Stable Isotope Laboratory. Values of $\delta^{13}\text{C}$ are reported relative to PDB and $\delta^{18}\text{O}$ values relative to SMOW. Reported precision is better than ± 0.05 per mil.
 6. R. S. Harmon, H. P. Schwarcz, D. C. Ford, D. L. Koch, *Geology* **7**, 430 (1979).
 7. To preserve the ornamentation of Cold Water Cave, we restored the stalagmite to its original position after coring.
 8. Preliminary U-Th ages were determined by alpha spectrometry at the University of Iowa. Powdered samples ranging from 0.6 to 2.1 grams were dissolved in 4 N HNO_3 by slow titration at room temperature, centrifuged, and separated from submilligram silicate residues. Samples were spiked with ^{228}Th - ^{232}U , and U and Th were purified by anion exchange chromatography. Counting times lasted 10 to 14 days, and counts were corrected for tailing and background contamination. Mass spectrometric analyses were performed at the Los Alamos National Laboratory. Samples of 0.2 to 0.9 grams were prepared by a method similar to alpha-dated samples with the use of 1.5 N HNO_3 for dissolution and spiked with ^{229}Th - ^{233}U - ^{236}U . The residue from the largest sample (MS-1) was analyzed for purposes of correction [T. L. Ku and Z. C. Liang, *Nuclear Instr. Methods Phys. Res.* **223**, 563 (1984)]. The ratio of ^{230}Th to ^{232}Th of the residue was 2.5×10^{-6} , a value typical for silicate rocks (for example, clay minerals). A National Bureau of Standards-designed, 30.5-cm radius, 90° deflection, single magnetic sector thermal ionization instrument equipped with ion counting detection systems was used to determine U concentrations and isotopic compositions. Measurements of Th were obtained on a similar instrument with two magnetic sectors in an "S" configuration. Details of the mass spectrometry procedure are described in S. J. Goldstein, M. T. Murrell, D. R. Janecky, *Earth Planet. Sci. Lett.* **96**, 134 (1989).
 9. C. H. Hendy, *Geochim. Cosmochim. Acta* **35**, 801 (1971).
 10. P. Fritz, R. J. Drimie, S. K. Frape, K. O'Shea, in *Proceedings of the International Symposium on Isotope Techniques in Water Resources Development* (International Atomic Energy Agency, Vienna, Austria, 1987), pp. 539-550.
 11. C. J. Yonge, D. C. Ford, J. Gray, H. P. Schwarcz, *Chem. Geol. Isot. Geosci. Sect.* **58**, 97 (1985).
 12. R. S. Harmon, *Water Resour. Res.* **15**, 503 (1979).
 13. L. A. González and K. C. Lohmann, in *Paleokarst*, N. P. James and P. W. Choquette, Eds. (Springer, New York, 1988), pp. 81-101.
 14. K. C. Lohmann, in *ibid.*, pp. 58-80.
 15. J. R. Gat, in *Proceedings of the International Symposium on Isotope Techniques in Water Resources Development* (International Atomic Energy Agency, Vienna, Austria, 1987), pp. 551-563.
 16. W. Dansgaard, *Tellus* **16**, 438 (1964).
 17. Y. Yurtsever and J. R. Gat, in *Deuterium and Oxygen 18 in the Water Cycle*, J. R. Ford and R. Gonfiantini, Eds. (International Atomic Energy Agency, Vienna, Austria, 1980), pp. 103-142.
 18. G. W. Moore and G. N. Sullivan, *Speleology* (Zephyrus, Teaneck, NJ, ed. 2, 1978).
 19. J. R. O'Neil, R. N. Clayton, T. J. Mayeda, *Chem. Phys.* **30**, 5547 (1969).
 20. B. Turi, in *Handbook of Environmental Isotope Geochemistry. The Terrestrial Environment, Part B*, P. Fritz and J. C. Fontes, Eds. (Elsevier, New York, 1986), pp. 207-238.
 21. T. E. Cerling, *Earth Planet. Sci. Lett.* **71**, 229 (1984).
 22. P. Deines, in *Handbook of Environmental Isotope Geochemistry. The Terrestrial Environment, Part A*, P. Fritz and J. C. Fontes, Eds. (Elsevier, New York, 1980), pp. 331-406.
 23. D. J. Ode and L. J. Tieszen, *Ecology* **61**, 1304 (1980).
 24. J. A. Teeri and L. G. Stowe, *Oecologia* **23**, 1 (1976).
 25. J. D. Hudson, *Geol. Soc. London* **33**, 637 (1977).
 26. K. L. Van Zant, *Quat. Res.* **12**, 358 (1979).
 27. R. G. Baker, C. A. Chumbley, P. M. Wittenok, H. K. Kim, *J. Iowa Acad. Sci.* **97**, 167 (1990).
 28. C. A. Chumbley, R. G. Baker, E. A. Bettis III, *Science* **249**, 272 (1990).
 29. Ages of pollen and plant macrofossil sites are routinely reported in radiocarbon years before present. We have converted radiocarbon years to years before present using data or figures (or both) in G. W. Pearson, J. R. Pilcher, M. G. L. Baillie, D. M. Corbett, and F. Qua [*Radiocarbon* **28**, 911 (1986)]; and in M. Stuiver, B. Kromer, B. Becker, and C. W. Ferguson [*ibid.*, p. 969].
 30. C. A. Chumbley, thesis, University of Iowa (1989).
 31. For the 25-year mean annual surface temperature over Cold Water Cave (7.3°C), Dansgaard's relation $\delta^{18}\text{O}_p = 0.695(t) - 13.6$ (16) yields a $\delta^{18}\text{O}_p$ value of -8.53 per mil, which is nearly identical to the $\delta^{18}\text{O}$ value for local shallow ground waters of -8.50 per mil (S. J. Kalkhof, personal communication).
 32. I. Friedman and J. R. O'Neil, in *U.S. Geol. Surv. Prof. Paper 440-KK* (1977).
 33. J. E. Kutzbach and T. Webb III, in *Quaternary Landscapes*, L. C. K. Shane and E. J. Cushing, Eds. (Univ. of Minnesota Press, Minneapolis, 1991), pp. 175-218.
 34. R. A. Bryson, *Geogr. Bull.* **8**, 228 (1966).
 35. W. L. Prell, J. V. Gardner, A. W. Be, J. D. Hays, *Geol. Soc. Am. Mem.* **145**, 247 (1976).
 36. W. H. Schlesinger, *Annu. Rev. Ecol. Syst.* **8**, 51 (1977).
 37. C. T. Rightmire and B. B. Hanshaw, *Water Resour. Res.* **9**, 958 (1973).
 38. P. J. Bartlein, T. Webb III, E. Fleri, *Quat. Res.* **22**, 361 (1984).
 39. W. A. Watts and R. C. Bright, *Geol. Soc. Am. Bull.* **79**, 855 (1968).
 40. R. G. Baker, L. J. Maher, C. A. Chumbley, K. A. Van Zant, *Quat. Res.* **37**, 379 (1992).
 41. J. H. McAndrews, *Mem. Torrey Bot. Club* **22**, 1 (1966).
 42. E. A. Bettis III, personal communication.
 43. We thank the Cold Water Cave owners K. and W. Flatland for granting access to the cave and M. Bounk, S. Barnett, P. Knoerr, and S. Moon for assistance. Supported by grants from the Littlefield fund and the Sedimentary Geochemistry Laboratory (to J.D.) and the Center for Regional and Environmental Research, University of Iowa (to L.G. and M.K.R.). Support for this research at Los Alamos National Laboratory was provided by a grant from the Geosciences Research Program (Department of Energy, Office of Basic Energy Science) (to M.T.M. and D.A.P.). Iowa Quaternary Studies Group Contribution 55.

13 July 1992; accepted 1 October 1992

Direct Detection of C_4H_2 Photochemical Products: Possible Routes to Complex Hydrocarbons in Planetary Atmospheres

Ralph E. Bandy, Chitra Lakshminarayan, Rex K. Frost, Timothy S. Zwier*

The photochemistry of diacetylene (C_4H_2), the largest hydrocarbon to be unambiguously identified in planetary atmospheres, is of considerable importance to understanding the mechanisms by which complex molecules are formed in the solar system. In this work, the primary products of C_4H_2 's ultraviolet photochemistry were determined in a two-laser pump-probe scheme in which the products of C_4H_2 photoexcitation are detected by vacuum ultraviolet photoionization in a time-of-flight mass spectrometer. Three larger hydrocarbon primary products were observed with good yield in the $\text{C}_4\text{H}_2^* + \text{C}_4\text{H}_2$ reaction: C_6H_2 , C_8H_2 , and C_8H_3 . Neither C_6H_2 nor C_8H_3 is anticipated by current photochemical models of the atmospheres of Titan, Uranus, Neptune, Pluto, and Triton. The free hydrogen atoms that are released during the formation of the C_6H_3 and C_8H_2 products also may partially offset the role of C_4H_2 in catalyzing the recombination of free hydrogen atoms in the planetary atmospheres.

Diacetylene (C_4H_2) plays a role in the stratospheres of several of the solar system's planets and moons analogous to that played by O_3 in Earth's atmosphere. The absorptions of C_4H_2 , like O_3 , serve as an effective ultraviolet radiation shield for the lower atmosphere and planetary surface. Yet, like O_3 , C_4H_2 is photochemically reactive (1) and is postulated as the primary source of yet larger hydrocarbons in these atmospheres (2-6). Despite the importance of C_4H_2 , the products of C_4H_2 photochemistry in the ultraviolet are not known. As a

result, the current photochemical models of Titan (2), Uranus (3), Neptune (4), Pluto (5), and Triton (6) postulate that C_8H_2 is the sole primary product of C_4H_2 's self-reaction. This report presents results of a photochemical study of C_4H_2 in which the primary photochemical products of the C_4H_2^* (excited state) + C_4H_2 reaction are unambiguously identified. Three primary products are observed with good yield: C_6H_2 (+ C_2H_2), C_8H_2 (+ H_2 , 2H), and C_8H_3 (+ H). Secondary products formed by subsequent reaction of the primary products with C_4H_2 are dominated by C_{10}H_3 and C_{12}H_3 .

The methods used to synthesize and handle C_4H_2 have been described (7). The

Department of Chemistry, Purdue University, West Lafayette, IN 47907.

*To whom correspondence should be addressed.